Remote Sensing of Environment 113 (2009) 82–93

Contents lists available at ScienceDirect

Remote Sensing of Environment

journal homepage: www.elsevier.com/locate/rse

Scaling and assessment of GPP from MODIS using a combination of airborne lidar and eddy covariance measurements over jack pine forests

L. Chasmer [a,*], A. Barr [b], C. Hopkinson [c], H. McCaughey [c], P. Treitz [a], A. Black [d], A. Shashkov [e]

[a] Department of Geography, Queen's University, Kingston ON, Canada K7L 3N6
[b] Climate Research Branch, Meteorological Service of Canada, Saskatoon SK, Canada S7N 3H5
[c] Applied Geomatics Research Group, Lawrencetown NS, Canada B0S 1M0
[d] Faculty of Land and Food Systems, University of British Columbia, Vancouver BC, Canada V6T 1Z4
[e] Climate Research Branch, Meteorological Service of Canada, Toronto ON, Canada M3H 5T4

ARTICLE INFO

Article history:
Received 21 November 2007
Received in revised form 19 August 2008
Accepted 22 August 2008

Keywords:
MODIS
Airborne lidar
Gross primary production
Forest
Eddy covariance
Scaling
Pixel heterogeneity

ABSTRACT

Understanding the influence of within-pixel land cover heterogeneity is essential for the extrapolation of measured and modeled CO_2 fluxes from the canopy to regional scales using remote sensing. Airborne light detection and ranging (lidar) was used to estimate spatial and temporal variations of gross primary production (GPP) across a jack pine chronosequence of four sites in Saskatchewan, Canada for comparison with the Moderate Resolution Imaging Spectroradiometer (MODIS) GPP product. This study utilizes high resolution canopy structural information obtained from airborne lidar to bridge gaps in spatial representation between plot, eddy covariance (EC), and MODIS estimates of vegetation GPP. First we investigate linkages between canopy structure obtained from measurements and light response curves at a jack pine chronosequence during the growing season of 2004. Second, we use the measured canopy height and foliage cover inputs to create a structure-based GPP model ($GPP_{Landsberg}$) which was tested in 2005. The GPP model is then run using lidar data (GPP_{Lidar}) and compared with eight-day cumulative MODIS GPP (GPP_{MODIS}) and EC observations (GPP_{EC}). Finally, we apply the lidar GPP model at spatial resolutions of 1 m to 1000 m to examine the influence of within-pixel heterogeneity and scaling (or pixel aggregation) on GPP_{Lidar}. When compared over eight-day cumulative periods throughout the 2005 growing season, the standard deviation of differences between GPP_{lidar} and GPP_{MODIS} were less than differences between either of them and GPP_{EC} at all sites. As might be expected, the differences between pixel aggregated GPP estimates are most pronounced at sites with the highest levels of spatial canopy heterogeneity. The results of this study demonstrate one method for using lidar to scale between eddy covariance flux towers and coarse resolution remote sensing pixels using a structure-based Landsberg light curve model.

© 2008 Elsevier Inc. All rights reserved.

1. Introduction

Ecosystem gross primary production (GPP) can be estimated at the flux footprint scale using eddy covariance (EC) methods (e.g. Barr et al., 2006) or over contiguous land cover types at the low resolution pixel scale using satellite-derived products from sensors such as the Moderate Resolution Imaging Spectroradiometer (MODIS) (e.g. Heinsch et al., 2006). However, reconciling local EC estimates of GPP from spatially and aerially variant flux footprints with fixed coverage satellite-based estimates poses a challenge that is a function of the disparate scales and methods of observation (e.g. Turner et al., 2002; Chen et al., 2008). In this paper, we aim to address part of this scaling problem by using canopy structural information extracted from airborne light detection and ranging (lidar) data to improve estimates of GPP both at the flux footprint and MODIS pixel scales.

A number of factors are known to lead to a level of incongruence between MODIS and site-specific (EC) estimates of GPP. These include: a) under-estimation of CO_2 exchanges by EC due to atmospheric stability, resulting in the apparent over-estimation of GPP by MODIS (e.g. Massman and Lee, 2002; Coops et al., 2007); b) scaling errors associated with comparing point measurements of GPP, leaf area index (LAI) and the fraction of photosynthetically active radiation absorbed by the canopy (fPAR) to large area remote sensing pixels (Tian et al., 2002; Turner et al., 2002; Turner et al., 2004; Heinsch et al., 2006); c) a limited ability to accurately represent the effects of three-dimensional canopy shadowing and ground surface reflectance on MODIS pixels (Xu et al., 2004; Eriksson et al., 2006; Jin et al., 2007); and d) MODIS pixel geolocation issues and the inclusion of land areas not represented by EC (Turner et al., 2004). Plot or transect measurements of vegetation characteristics, used to rectify these issues within large area MODIS pixels, are also often difficult and time-consuming to obtain, especially in remote locations (Heinsch et al., 2006).

* Corresponding author.
E-mail address: lechasme@yahoo.ca (L. Chasmer).

0034-4257/$ – see front matter © 2008 Elsevier Inc. All rights reserved.
doi:10.1016/j.rse.2008.08.009

Table 1
Average vegetation characteristics at OJP, HJP75, and HJP94 for 22 plots

Site	Number of trees sampled	Average stem density (stems m^{-2})	Average tree height (m)	Average DBH* (cm)	Average fractional cover	Average canopy depth (m)	Average crown diameter (m)	Other species
OJP	381	0.11 (0.001)	14.2 (3.5)	9.33 (4.55)	0.59 (0.06)	8.3 (2.7)	2.0 (1.0)	Alder, bearberry, reindeer lichen, blueberry, cranberry
HJP75	1447	0.59 (0.19)	6.3 (1.6)	5.69 (3.49)	0.57 (0.06)	3.5 (1.3)	0.9 (0.4)	Grasses, reindeer lichen, bearberry
HJP94	2081	0.86 (0.56)	1.6 (0.7)	2.31 (1.05)	0.16 (0.11)	1.6 (0.7)	0.7 (1.1)	Grass, blueberry, alder, raspberry, bearberry, reindeer lichen

The values in parentheses represent standard deviation.
* DBH refers to tree bole diameter at breast height (1.3 m above the ground).

We believe that some of the challenges associated with comparing EC estimates of GPP with fixed coverage MODIS pixel-based estimates can be addressed by scaling between these disparate observation methods using airborne lidar data. Lidar provides a very high resolution map of the three-dimensional characteristics of the vegetated canopy, understory, and ground surface. The interception of photosynthetically active radiation (PAR) by the canopy and understory directly impacts GPP and photosynthesis (e.g. Baldocchi and Meyers, 1998) through the convergence efficiency of intercepted PAR to GPP, also known as light use efficiency (LUE) (Turner et al., 2002; Schwalm et al., 2006). LUE can be estimated from the slope of a Landsberg light response curve, which is related to the saturation of photosynthesis beyond certain light levels (e.g. Turner et al., 2002; Turner et al., 2003). If LUE for an ecosystem is known or can be estimated from a look-up table, for example, then the Landsberg curve can be used to model GPP:

$$\mathrm{GPP}_{\mathrm{Landsberg}} = P_{\max}\left(1-e^{-\alpha\left(\mathrm{PAR}-I_{\mathrm{comp}}\right)}\right), \quad (1)$$

where $P_{\max}$ is the maximum average GPP at saturation (g C m^{-2}) (the point at which GPP plateaus with increased light levels), α is the slope or scaling factor of GPP as it increases with incoming PAR, and I_{comp} is the light compensation point at which GPP is zero. This then provides the context for scaling between EC and MODIS using airborne lidar. EC estimates of GPP are based on measures of flux from the ecosystem, and MODIS estimates of GPP are based on the absorption and reflection of light from within ~1 km resolution pixels. However, actual canopy detail is not considered. In both cases (EC and MODIS) the canopy and understory structure is implicit in directly influencing the GPP estimate. Lidar enables this implicit treatment of canopy structure to be made explicit in both cases.

A hypothesis can be formulated as follows: Foliage density and canopy height, which can be estimated from lidar, may correspond with variability in LUE. LUE is also used in the MODIS algorithm to estimate GPP. To illustrate that LUE and GPP may be related to canopy structure, an example is provided: papers by Schwalm et al. (2006) and Chen et al. (2006) have recorded LUE, canopy height and fractional cover (as fPAR) for the same 16 Fluxnet-Canada forest sites. Comparing the observations from both papers, we find that average growing season LUE for boreal conifer and deciduous forests, temperate rain forest, previously harvested stands, and previously burned stands is significantly related to average canopy height (r^2=0.61, p=0.001, RMSE=0.19 g C MJ^{-1} APAR (not shown)) (see Schwalm et al., 2006). Based on this comparison and results in Chasmer et al. (2008) and Chasmer et al. (accepted for publication) it follows that (all else being equal) areas displaying taller canopy heights and/or fractional canopy cover will be positively related to gross photosynthesis and CO_2 uptake. Therefore, Landsberg input parameters, such as average maximum GPP, may be greater for canopies containing more biomass and taller trees. The light compensation point may also vary due to within canopy shadowing, fractional cover and vegetation height. For example, shorter vegetation with lower fractional cover will receive more radiation early in the morning than taller vegetation with greater fractional cover (due to long morning shadows), thereby increasing the level of light required for photosynthesis in forests of taller trees and greater leaf area. If this is the case, then GPP may be modeled using the Landsberg curve, canopy height and fractional cover estimates from airborne lidar.

The analysis presented first investigates linkages between field-based canopy structure measurements and Landsberg light response curves at a jack pine chronosequence during the growing season of 2004 and tested in 2005 ($\mathrm{GPP}_{\mathrm{Landsberg}}$). Second, we use the lidar inputs (fractional cover and canopy height) to create a structure-based GPP model ($\mathrm{GPP}_{\mathrm{lidar}}$) (also tested in 2005). $\mathrm{GPP}_{\mathrm{lidar}}$ is then compared with eight-day cumulative MODIS GPP ($\mathrm{GPP}_{\mathrm{MODIS}}$) and EC observations ($\mathrm{GPP}_{\mathrm{EC}}$). Finally, we apply $\mathrm{GPP}_{\mathrm{lidar}}$ at spatial resolutions of 1 m to 1000 m at three jack pine sites to examine the influence of within-pixel heterogeneity and scaling (or pixel aggregation) on modeled GPP.

2. Data collection

2.1. Site characteristics

Four jack pine sites, forming a post-harvest chronosequence, were examined during the growing seasons (June 1st to September 31st) of 2004 and 2005. The jack pine stands included a mature jack pine forest of ~90 years of age (OJP); an immature jack pine forest harvested in 1975 (HJP75); a regenerating jack pine forest harvested in 1994 (HJP94); and a naturally regenerating jack pine site harvested in 2000 and scarified in 2002 (HJP02). The forest stands are located within 6 km of each other near the southern edge of the boreal forest, north of Prince Albert, Saskatchewan, Canada. All sites examined in this study were operating as part of Fluxnet-Canada (Barr et al., 2006; Margolis et al., 2006), under the Boreal Ecosystem Research and Monitoring Sites (BERMS) project. Each site is relatively flat with coarse-textured and well-drained sandy soils (e.g., Baldocchi et al., 1997).

Forest stand characteristics are summarized in Tables 1 (OJP, HJP75, and HJP94) and 2 (HJP02). Measurements of canopy structure were made at eight (OJP), eight (HJP75), and six (HJP94) geo-located 11.3 m radius plots located at distances of 100 m and 500 m (at OJP and HJP75) and within 250 m (HJP94) of EC towers in May and August, 2005. At HJP02, four 25 m×2 m transects containing 50 1 m×1 m plots

Table 2
Average vegetation characteristics at HJP02 for 200 1 m×1 m plots along four transects

Number of trees (in 200 1 m plots)	Average tree height (stdev) (m)	Average % tree cover (stdev)	Average % grass cover (stdev)	Average % reindeer lichen cover (stdev)	Average % soil cover (stdev)	Average % wood debris cover (stdev)	Average % herb cover (stdev)	LAI from PAR ($m^2 \cdot m^{-2}$)
37	0.19 (0.12)	9 (11)	21 (18)	23 (30)	32 (18)	26 (24)	8 (15)	0.29

Average percent cover does not add up to 100% (averaged between four transects) because some plots have differing amounts of individual coverage types. Values in parentheses represent standard deviation.

were located at distances of 50 m to 75 m (N, S, E, and W) from the EC tower. The centre of plots, and the start and end of transects were located using survey-grade, differentially corrected global positioning system (GPS) receivers (Leica SR530, Leica Geosystems Inc. Switzerland; Ashtec Locus, Ashtec Inc., Hicksville, NY) with the same base station coordinate as was used for the lidar survey. Geo-location accuracies varied from 1 cm to 1 m depending on the canopy cover density at the time of GPS data collection.

Canopy gap fraction was obtained using digital hemispherical photography (DHP) at OJP, HJP75, and HJP94, and radiation sensors at HJP02 (Chasmer et al., 2008). One photograph was taken at the centre of the plot, and four were located 11.3 m from the centre along cardinal (N, S, E, and W) directions, determined using a compass bearing and measuring tape (Fluxnet-Canada, 2003). Photographs were taken at a height of ~1.3 m at OJP and HJP75, and 0.7 m at HJP94. Trees were often less than 2 m in height at HJP94; therefore a lower DHP height was chosen to capture more biomass. Photographs were taken during either diffuse daytime conditions, or 30 min before dawn or after dusk, at one F-stop below normal exposure. Under-exposure of photographs reduces the influence of sun brightness and under-estimation of leaf area (Zhang et al., 2005). Individual photographs were processed following sky and vegetation thresholding methods of Leblanc et al. (2005). Thresholds for sky and foliated pixels were used to obtain estimates of gap fraction (Ω) within the software, DHP version 1.6.1 (S. Leblanc, Canada Centre for Remote Sensing provided to L. Chasmer through the Fluxnet-Canada Research Network). Average canopy height, estimated using a Vertex sonic hypsometer (Haglof, Maddison), and vegetation fractional cover ($1-\Omega$) per site were compared with inputs used in light response curves, whereas plot level averages were compared with lidar estimates of the same.

2.2. Site instrumentation

Measurement and processing of eddy covariance (EC) data has been discussed in Kljun et al. (2006) and Barr et al. (2006) and follow Fluxnet-Canada procedures for standardization between sites. Briefly, EC was used at all sites to measure CO_2 fluxes averaged over 30-minute periods and then aggregated on a daily basis and again, over eight day periods for comparison with MODIS. The plot measurement-based GPP model ($GPP_{Landsberg}$) was developed using EC data collected during the growing season (June 1st to September 31st) of 2004 and was then tested and compared with GPP_{EC} and GPP_{MODIS} in 2005.

GPP (used interchangeably with gross ecosystem production, GEP) was estimated from EC-measured net ecosystem production (NEP) (μmol m^{-2} s^{-1}) and modeled ecosystem respiration (Re) (μmol m^{-2} s^{-1}). Re was estimated based on the relationship between nighttime Re and soil temperature (Barr et al., 2004). Cumulative daily estimates of GPP_{EC} have been expressed in units of g C m^{-2} day^{-1} for direct comparison with GPP_{MODIS} (kg C m^{-2} 8-days^{-1} converted to g C m^{-2} 8-days^{-1}). CO_2, H_2O and friction velocity were measured using a sonic anemometer (CSAT3, Campbell Scientific Inc. Edmonton, Alberta, Canada at OJP and HJP02; Gill R3-50, Gill Instruments Ltd., England at HJP75; SAT-550, Kaijo Co., Tokyo, Japan at HJP94) combined with a closed path infrared gas analyzer (LI 6262, LI-COR Inc., Lincoln, NE, USA). EC systems have been installed above the canopy at heights of approximately 28 m, 17 m, 3 m, and 2 m at OJP, HJP75, HJP94, and HJP02 respectively. Any gaps in the 30-minute fluxes were filled using a moving-window regression approach (Barr et al., 2006; Kljun et al., 2006). EC data were quality controlled using a minimal surface friction velocity of 0.35 m s^{-1} at all sites, and an energy balance closure correction was applied to reduce under-estimates of measured net ecosystem exchange (NEE) by EC (Barr et al., 2006).

Above-canopy incoming and reflected PAR (400 to 700 nm) and below-canopy incoming PAR were measured using quantum sensors LI-COR model LI190 at OJP and HJP75 (LI-COR Biosciences, Nebraska, USA); and Eko model ML-020P (Eko Instruments, Co. Ltd., Japan) at HJP94 and HJP02. Above canopy incident and reflected PAR sensors were installed on booms at heights of 28 m, 12 m, 3 m and 2 m above the ground at OJP, HJP75, HJP94, and HJP02. Below canopy incident PAR measurements were made at OJP and HJP75 at a height of ~1 m. Below-canopy PAR measurements were not available at HJP94 and HJP02.

2.3. Lidar data collection and analysis

Airborne lidar data were obtained throughout the entire White Gull River watershed, including jack pine chronosequence sites, on August 12, 2005. The lidar system is an Airborne Laser Terrain Mapper (ALTM) 3100 (Optech Inc. Toronto, Ontario, Canada) small-footprint discrete pulse return lidar. Data were collected in partnership with the Applied Geomatics Research Group (AGRG), Nova Scotia, Canada. The lidar was flown at a height of 950 m above the ground surface, and emitted laser pulses at a rate of 70 kHz. A ±19° scan angle was used with 50% overlap of scan lines, enabling penetration of laser pulses through to the base of the canopy and returns from all sides of individual trees (Chasmer et al., 2006). Up to four laser returns were obtained per laser pulse emitted resulting in cross- and down-track resolutions of ~35 cm.

After initial processing of GPS trajectories and range files at the AGRG, lidar data were imported into the software package Terrascan (Terrasolid, Finland) for area subsetting and laser return classification. The larger lidar dataset was subset into 1 km × 1 km areas containing EC flux stations within the same geographical area covered by one MODIS pixel. Circular 11.3 m radius mensuration plots were also extracted from the lidar for comparison with average plot-measured canopy height and fractional cover. Lidar datasets were then filtered for outlying returns greater than the height of the EC tower or lower than 1.5 m below the ground surface. Datasets were then classified into "ground" returns (P_{ground}), "canopy" returns (above 1.3 m at OJP and HJP75; and 0.7 m at HJP94) (P_{canopy}), and "all" returns (which included ground returns) (P_{all}). P_{ground} was used to create a 2 m × 2 m digital terrain model (DTM) from which P_{all} and P_{canopy} returns were normalized relative to the ground surface. The DTM was created by interpolating between ground returns within 2 m resolution pixels using an inverse distance weighting procedure (IDW) (i.e. O'Sullivan and Unwin, 2003) and a search radius of 3 m. This method was chosen because it a) retains point values of the data; b) is a rapid interpolation method, which is important when dealing with large volumes of lidar data; and c) is appropriate for regularly spaced data (Myers, 1994). Although the resolution of the lidar dataset is greater than 2 m, areas of dense canopy foliage and individual alder bushes can reduce the density of ground returns. Therefore a 2 m resolution was used to avoid "holes" within the DTM.

Lidar canopy height models (CHM) were created from the normalized maximum z-height (m) at jack pine sites using IDW at 1 m × 1 m resolution. At HJP02, short vegetation and ground topography could not be resolved between first, intermediate, and last returns. This is due to the inability of lidar systems to distinguish between returns separated by less than 1.6 m, depending on the lidar systems used (Hopkinson et al., 2005). Therefore, comparisons at HJP02 were limited to measured data only and did not include any lidar data analysis. Fractional cover (*f*cover) (where 1 = full canopy cover and 0 = no canopy cover) was estimated based on the ratio of the number of canopy returns to the number of all returns within 1 m × 1 m × height columns throughout each site:

$$f\text{cover} = \left(\frac{\sum P_{\text{canopy}}}{\sum P_{\text{all}}}\right). \tag{2}$$

The *f*cover or "return ratio" method has been examined in various forms within numerous studies and closely approximates fractional cover when compared with DHP (Morsdorf et al., 2006; Solberg et al., 2006; Hopkinson and Chasmer, in review).

2.4. MODIS GPP product

GPP_{MODIS} (Collection 5) data were obtained from the Oak Ridge National Laboratory (ORNL) Distributed Active Archive Center (DAAC) (http://www.modis.ornl.gov/modis/index.cfm) and was subset into 3 km × 3 km areas (9 pixels) at OJP, HJP75, HJP94 and HJP02 flux tower sites. Eight-day cumulative periods were compared with the same cumulated GPP periods observed from EC. Only days that contained the best quality controlled MODIS data for all nine pixels were included. The estimation of GPP by MODIS is described in detail in Running et al. (1999), Zhao et al. (2005), and Heinsch et al. (2006).

3. Methods

In this study, four methods are used to estimate GPP. These include EC (GPP_{EC}), Landberg curves based on local plot measurements ($GPP_{Landsberg}$), Landsberg curves based on airborne lidar (surrounding the EC) within the area covered by one MODIS pixel (GPP_{lidar}), and MODIS pixel estimates containing the EC (GPP_{MODIS}). $GPP_{Landsberg}$ has been modeled in 2004 and tested and compared in 2005. Table 3 provides a summary of the four methods that are used. Further discussion of the methodologies used to define these estimates is found in the following sections.

3.1. Objective 1: Landsberg light response curve analysis and development of GPP model

The first objective makes comparisons between Landsberg input variables used to predict GPP from light response curves and canopy structure attributes at the jack pine chronosequence during the growing season of 2004. The purpose is to first determine if there is a relationship between canopy structure and Landsberg input variables, and if there is, to then develop GPP models based on canopy structure and Landsberg principles.

The Landsberg Eq. (1) (e.g. Landsberg and Waring, 1997; Chen et al., 2002) was used to examine the relationships between daily average incoming PAR and GPP_{EC} per site during 2004. Fitted values for P_{max} and α were compared to canopy height across sites and the fitted value for I_{comp} was compared with average fractional cover across sites to estimate GPP ($GPP_{Landsberg}$). However, fractional cover was not actually measured in 2004. To estimate fractional cover in 2004, DHP plot measurements were adjusted based on percentage differences in fractional cover measurements made by PAR sensors between 2004 and 2005:

$$\text{Fractional cover} = (\text{PAR}_{AC\downarrow} - PAR_{BC\downarrow})/\text{PAR}_{AC\downarrow}, \tag{3}$$

and at HJP94 and HJP02:

$$\text{Fractional cover} = \text{PAR}_{AC\downarrow}\left(1 - e^{-kL^*}\right)/\text{PAR}_{AC\downarrow} \tag{4}$$

where $PAR_{AC\downarrow}$ is above-canopy incoming PAR, and $PAR_{BC\downarrow}$ is incoming below-canopy PAR after interception with branches and leaves. L is LAI, and k is the extinction coefficient estimated as a constant 0.45 for simplicity (Chen et al., 2006). Measured fractional cover [3, 4] was examined during diffuse radiation conditions only and then averaged throughout the growing season. Based on results of Middleton et al. (1997) we have assumed that canopy fractional cover did not vary at the jack pine sites within the growing seasons studied.

Measured below canopy PAR percent differences between the two years were used to vary site-averaged estimates of fractional cover between 2004 and DHP measurements in 2005. PAR adjusted DHP fractional cover was estimated as 0.57 (OJP), 0.73 (HJP75), 0.41 (HJP94), and 0.22 (HJP02) in 2004. Measurement of average fractional cover by DHP was 0.59 (OJP), 0.72 (HJP75), 0.39 (HJP94) and 0.29 (HJP02) in 2005. Meteorological conditions during 2004 were similar to 2005; however, a severe drought in 2003 and a late, cool spring in 2004 may have caused slight reduction in foliage cover at some sites (Chasmer et al., 2008).

Tree heights also were not measured in 2004 and were estimated based on jack pine forest growth rates in Manitoba and Saskatchewan (Burns and Honkala, 1990). Average growth rates are approximately 0.15 m from ages one to two, 0.23 m per year from ages five to eight years, 0.33 m per year at age 30, and 0.23 m per year at age 50. Canopy heights for 2004 were reverse estimated and averaged from the 2005 field plot data as 13.97 m (OJP), 5.64 m (HJP75), 1.37 m (HJP94), and 0.15 m (HJP02).

3.2. Objectives 2: GPP model assessment

GPP was modeled based on the relationships between canopy height and fractional cover, and Landsberg curve inputs in 2004. To test the applicability of the model, the structure-based GPP model was run during the 2005 growing season by substituting 2005 measured canopy height and fractional cover, and incoming PAR into the Landsberg equations ($GPP_{Landsberg}$). $GPP_{Landsberg}$ was then compared with GPP_{EC} in 2005.

Root mean square error (RMSE), systematic RMSE ($RMSE_s$) and unsystematic RMSE ($RMSE_u$) were used to evaluate the accuracy of $GPP_{Landsberg}$ when compared with GPP_{EC}. RMSE provides a measure of the average differences between observed and predicted GPP, whereas $RMSE_s$ and $RMSE_u$ provide measures of the systematic biases and unsystematic or random biases un-related to the model (Rymph, 2004). $RMSE_s$ and $RMSE_u$ were calculated as:

$$\text{RMSE}_s = \sqrt{\frac{\sum_{i=1}^{n}\left(\hat{P}_i - O_i\right)^2}{n}} \tag{5}$$

and

$$\text{RMSE}_u = \sqrt{\frac{\sum_{i=1}^{n}\left(P_i - \hat{P}_i\right)^2}{n}} \tag{6}$$

where O_i is the GPP_{EC}, P_i is the $GPP_{Landsberg}$, $P_i = mO_i + b$, and m and b are the slope of the regression lines and Y-intercepts, respectively

Table 3
Summary of GPP methods estimated using EC, plot measurements, airborne lidar, and MODIS

GPP estimation method	Description	Growing season examined	Data inputs
GPP_{EC}	GPP estimated using EC	2004 and 2005. 2005 compared with all other GPP methods.	NEE, Re
$GPP_{Landsberg}$	GPP estimated using canopy structure inputs from forest plot measurements	Method developed in 2004, tested in 2005. 2005 compared with all other GPP methods.	Incoming PAR, average measured tree height and fractional cover
GPP_{lidar}	GPP estimated using area averaged canopy height and fractional cover from airborne lidar. Average areas include that within MODIS pixel area including the EC (1 km × 1 km)	2005 compared with all other GPP methods.	Incoming PAR, lidar average tree h eight and fractional cover
GPP_{MODIS}	GPP estimated from MODIS within the pixel containing the EC at each site.	2005 compared with all other GPP methods.	Incoming PAR, MODIS fPAR product, and LUE determined from a look-up table.

Table 4
Parameters (P_{max}, I_{comp}, and α) used in Landsberg curves and the correlation between incoming PAR and GPP described by the Landsberg curve

Site	P_{max} (μmol m^{-2} s^{-1})	α (scaling)	I_{comp} (μmol m^{-2} s^{-1})	Correlation (r^2) between incoming PAR and GPP described by Landsberg curve
OJP	10.37	0.0048	12	0.60
HJP75	9.25	0.0035	14	0.54
HJP94	6.53	0.0028	10	0.61
HJP02	1.71	0.0011	8	0.08

Landsberg input parameters have been determined from all 30-minute periods of PAR and GPP measured during the growing season of 2004.

(from Rymph, 2004). Models that perform well have low RMSE, $RMSE_s$ should be close to zero and the $RMSE_u$ should be close to the RMSE. Low measurements of $RMSE_s$ indicate that the model is predicting at maximum accuracy and the sources of errors are random and not related to the model (Rymph, 2004).

3.3. Objective 3: model application and comparison

The third objective uses airborne lidar to spatially model GPP (GPP_{lidar}) within the 1 km×1 km area surrounding the EC station (equivalent to one MODIS pixel) at 1 m resolution during the growing season of 2005. Average canopy height from the CHM and lidar fractional cover (*f*cover) are input into the Landsberg GPP model (Objective 1) to estimate GPP (GPP_{lidar}). GPP_{lidar} is compared with GPP_{MODIS} and GPP_{EC}, cumulated over 8-day periods during the growing season of 2005. The purpose is to compare GPP_{lidar} at the MODIS pixel scale with GPP_{EC} at the flux footprint scale and GPP_{MODIS} at 1 km resolution to determine if differences in GPP exist as a result of spatial variability in canopy structure beyond the footprint of the EC station. We hypothesize that GPP_{Lidar} and GPP_{MODIS} will be more similar than when compared with GPP_{EC} because the same area will be included in the estimation of GPP using remote sensing methods, whereas GPP_{EC} will sample a smaller area within the larger MODIS pixel. The maximum source area of the footprint extends to up to 1 km at OJP and HJP75, 250 m at HJP94, and 150 m at HJP02 during convective daytime periods (Chasmer et al., accepted for publication).

3.4. Objective 4: GPP scaling analysis

The final objective aggregates GPP_{lidar} from 1 m to 25 m, 250 m, 500 m, and 1000 m resolutions to determine the influence of within pixel patches on GPP estimation. This is done by averaging from higher resolution pixels (i.e. 1 m) to lower resolutions in ArcGIS (ESRI, CA). When scaling from 1 m to 25 m resolution, for example, the mean of all 1 m resolution pixels within the 25 m×25 m area are used to estimate a single value of GPP at 25 m resolution. This was repeated for all pixels within each MODIS pixel area (i.e. 1 km×1 km). The same methodology was then applied to other resolutions by aggregating all 1 m×1 m pixels within 250 m×250 m, 500 m×500 m, and 1000 m×1000 m pixels by retaining the individual 1 m resolution cell values of GPP. The mean GPP_{lidar} of the lower resolution pixels was used following results of Woolard and Colby (2002). They found that the means of the aggregated pixels were statistically most appropriate when compared with other methods of aggregation (i.e. central pixel resampling, median, etc.) and retained patterns in the landscape at varying scales. Comparisons between resolutions were then made by subtracting each lower resolution pixel from 1 m×1 m pixels.

4. Results

4.1. Objective 1: comparisons between Landsberg inputs and canopy structure

Incoming PAR accounted for 60%, 54%, 61% and 8% of the variability of 30-minute average GPP_{EC} at OJP, HJP75, HJP94, and HJP02 (Table 4, Fig. 1). Landsberg curve relationships between GPP_{EC} and incoming PAR indicate that saturation occurred at different levels of PAR depending on the forest age and the structural characteristics of the site. This indicates that canopy structure plays a role in the variability in CO_2 uptake per site,

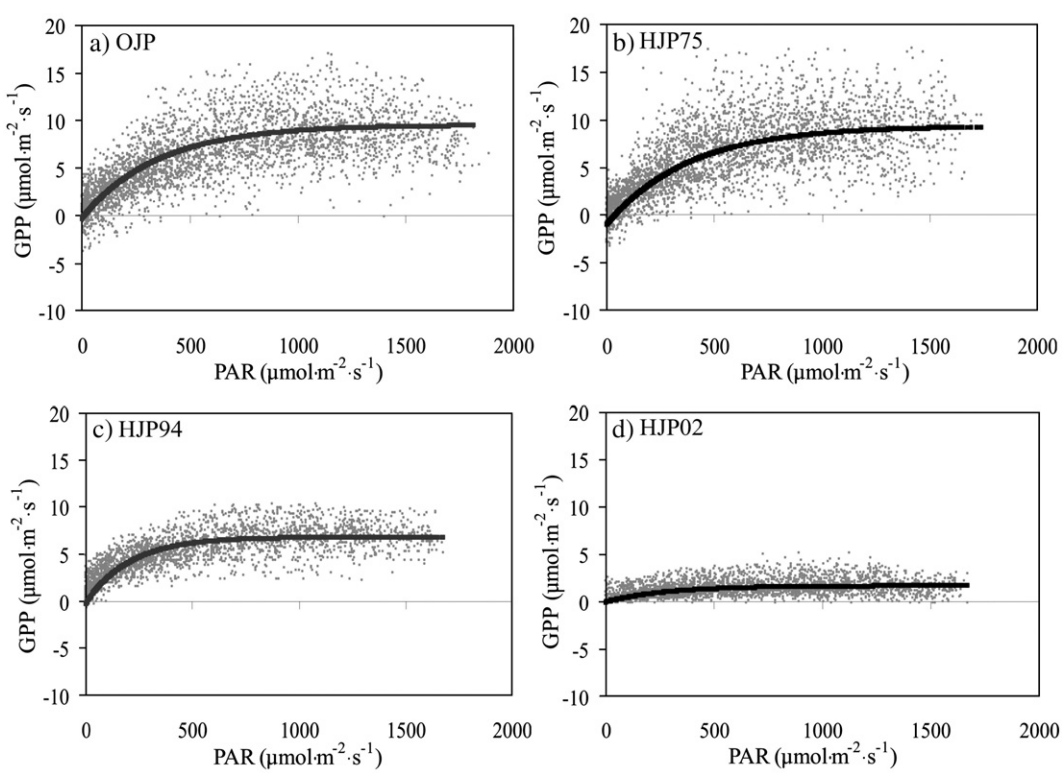

Fig. 1. Landsberg model light response curves and relationships between observed 30-minute incoming PAR (μmol m^{-2} s^{-1}) and GPP (μmol m^{-2} s^{-1}) during the 2004 growing season.

and the non-linearity of the Landsberg curves. GPP saturated at incoming PAR levels of approximately 800, 700 and 450 μmol m^{-2} s^{-1} at OJP, HJP75, HJP94 and almost immediately at HJP02.

Relationships between average measured tree heights, measured fractional cover and Landsberg input variables are shown in Fig. 2 for 2004. P_{max} was positively related to average canopy height (r^2=0.99), where taller trees had greater average maximum GPP at saturation than shorter trees at the sites studied. The relationship was non-linear, where increases in P_{max} with height were greatest between HJP02 and HJP94, and leveled off between HJP75 and OJP. Relationships between P_{max} and fractional cover were lower, but still non-linear (r^2=0.74). I_{comp} was linearly related to the average fraction of foliage cover within each stand (r^2=0.99) and non-linearly related to canopy height (r^2=0.80). The scaling function (α) also varied with canopy structure (r^2=0.97, canopy height; 0.68, fractional cover). α was greatest at OJP and was slightly lower at HJP75 and HJP94. At HJP02, the scaling function was much lower than at other sites.

Based on the relationships between plot measured canopy structure (Table 1) and Landsberg input variables (Fig. 2), canopy structure obtained either from plot measurements may be used to model GPP. P_{max}, I_{comp}, and α can be substituted into the Landsberg equation (including daily incoming PAR) based on logarithmic and linear relationships between sites as follows:

$$P_{max} = 2.8 \times Ln(\text{tree height}) + 6.50, \quad (7)$$

$$I_{comp} = 13.7 \times (\text{fraction cover}) + 5.17, \quad (8)$$

and

$$\alpha = 0.0008 \times Ln(\text{tree height}) + 0.0026. \quad (9)$$

Application of these relationships is suitable only for the sites examined in this study. Relationships between measured canopy structure and Landsberg inputs should be examined at other sites.

4.2. Objective 2: comparing GPP predicted from height and fractional cover with GPP_{EC}

In the second objective, $GPP_{Landsberg}$ [Eqs. (7), (8), and (9)], is tested and compared with GPP_{EC} during the 2005 growing season at each site. Average canopy cover and tree heights from plot measurements were used to estimate $GPP_{Landsberg}$ (Table 3; Fig. 3).

$GPP_{Landsberg}$ (Table 5) compared well with GPP_{EC} at all sites but HJP02 in 2005. The slopes of the linear regression (ideally 1.00) were between 0.72 and 0.78 at OJP, HJP75, and HJP94. The Y-intercept was close to zero at HJP94 and HJP02, but high at OJP and HJP75 (2.28 g C m^{-2} d^{-1}, and 1.31 g C m^{-2} d^{-1}). This indicates that $GPP_{Landsberg}$ was over-estimated at OJP and HJP75 for low values of GPP_{EC}. Table 5 provides measures of $GPP_{Landsberg}$ model accuracy when compared with GPP_{EC}. Examination of daily GPP_{EC} using probability plots (not shown) indicate that OJP and HJP02 were normally distributed in 2004, whereas HJP75 and HJP94 were not normally distributed. In 2005, when the model was tested, OJP, HJP75, and HJP94 were normally distributed, whereas HJP02 was not. Either Pearson's *r* or Spearman's rank correlations are shown for each site because Pearson's r correlation requires that data are normally distributed, whereas Spearman's rank does not. Daily RMSE was less than 10% of the mean daily GPP, and systematic errors varied by less than ~14% of the mean daily GPP at HJP75, HJP94, and HJP02. Unsystematic errors were lower than systematic errors at all sites, except HJP75, indicating that predicted GPP may have been influenced by other factors at this site. At OJP, however, the model did not perform as well, indicating that predicted GPP was prone to some systematic biases and could be further refined.

4.3. Objective 3: comparing GPP_{EC} with GPP_{MODIS} and GPP_{lidar}

Airborne lidar provided reasonable estimates of canopy fractional cover (based on annulus rings 1–9) at 40, 40, and 30 DHP locations within OJP, HJP75, and HJP94, respectively. Correlations (r^2) between measured vs. lidar *f*cover were 0.86 for all DHP plots combined. Due to

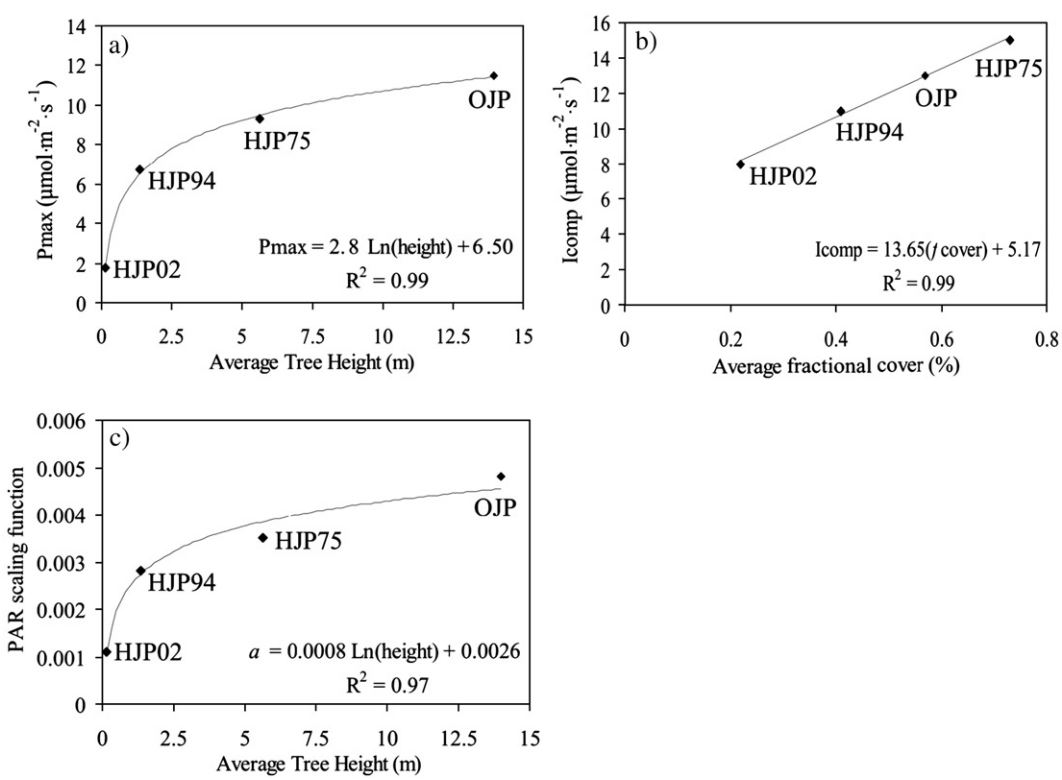

Fig. 2. Site-level relationships between a) P_{max} and average measured tree height; b) I_{comp} and average measured fractional foliage cover from DHP; and c) α and average measured tree height estimated in 2004.

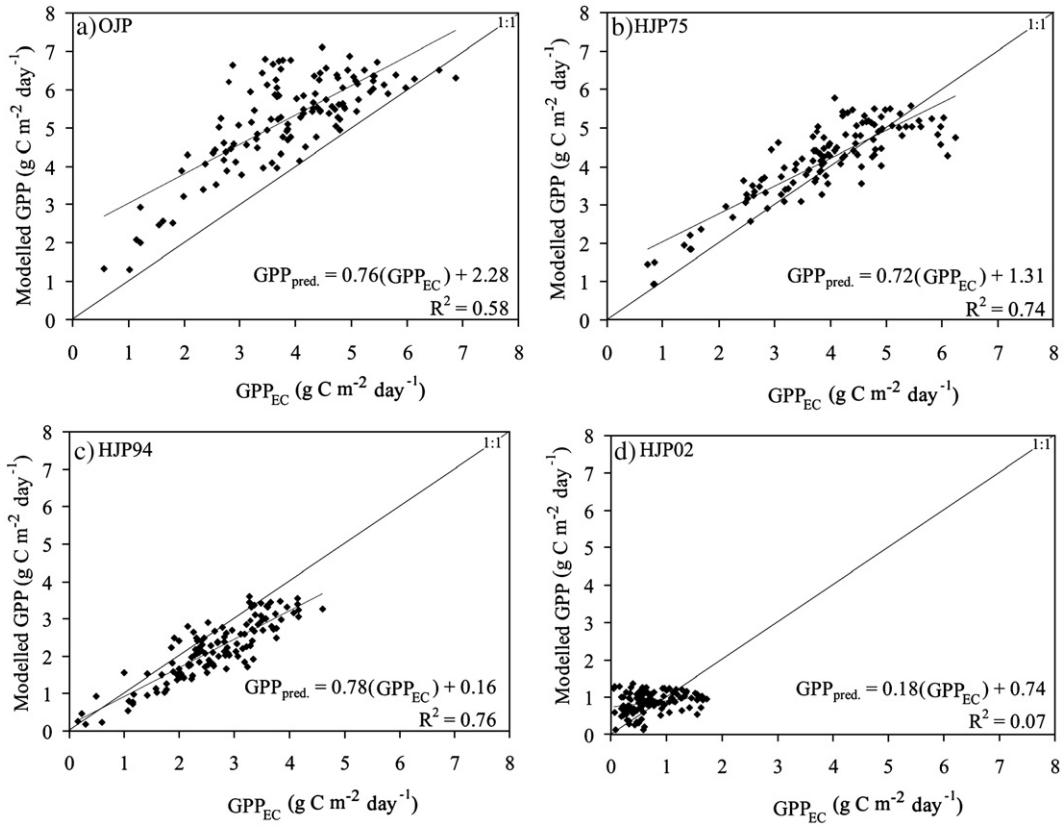

Fig. 3. Comparisons between GPP_{EC} and $GPP_{Landsberg}$ with the inclusion of measured canopy height and fractional cover during the growing season of 2005.

reduced variance for individual forest cover types, however, the site-specific (OJP, HJP75, and HJP94 (HJP02 has been excluded)) lidar and DHP fractional cover correlations were not as strong (r^2=0.22 (p=0.01), 0.09 (p<0.1), and 0.21 (p=0.01), respectively). This indicates that the *f*cover method works well over variable canopy structures, but not as well within a single ecosystem of little variability. Average percent differences between measured and lidar-estimated *f*cover were 19% (standard deviation (stdev.)=9%, OJP), 15% (stdev.=9%, HJP75) and 36% (stdev.=22%, HJP94). Comparisons between plot-averaged measured tree height and lidar canopy heights, based on the 90th percentile of the return distribution, were strong (r^2=0.99) and followed an almost 1:1 relationship. Site-specific correlations were also strong at OJP (r^2=0.88) and HJP75 (r^2=0.83), but were weak at HJP94 (r^2=0.18, p=0.32). This was due to the low height of the trees at HJP94 resulting in reduced probability of multiple returns and increased penetration of pulses into surrounding tall grasses and shrubs (Hopkinson et al., 2005). From the results presented here and elsewhere, lidar can provide a map of the spatial variability of canopy height (e.g. Hopkinson et al., 2005) and *f*cover (e.g. Morsdorf et al., 2006) for use in the Landsberg-based GPP model over large areas.

Direct comparisons between GPP_{EC}, GPP_{MODIS}, and GPP_{lidar} are shown in Fig. 4. Adjacent MODIS pixels provide maximum and minimum ranges (as error bars) of GPP and were used as bounds for geo-location errors that occur as a result of sensor geometry, earth curvature, and ground surface topography (e.g. Wolfe et al., 2002; Turner et al., 2004).

Mixed pixels may have had some influence on the relationships between GPP_{EC}, GPP_{lidar}, and GPP_{MODIS} (Fig. 4). Table 6 provides Pearson's r correlation coefficients between GPP_{EC}, GPP_{lidar} and GPP_{MODIS} and the average percent difference when compared with each other for all sites examined. OJP is relatively homogeneous throughout the entire MODIS pixel. Lidar estimated average (1 km×1 km area surrounding the EC) *f*cover was 0.62 (slightly higher than measured, 0.59) and average canopy heights were much lower than that measured at plots (11.2 m) (Table 1). At OJP, GPP_{lidar} underestimated eight-day total GPP_{EC} by 11%, whereas GPP_{MODIS} underestimated eight-day total GPP_{EC} by 6%, on average (Fig. 4, Table 6). The differences may have been due, in part, to shorter average vegetation heights within the larger MODIS pixel as opposed to taller trees within the footprint of the EC system.

At HJP75, average lidar canopy height and *f*cover (5.67 m, 0.47) were lower than plot measurements (Table 1), which may have caused some underestimation of GPP_{lidar} (6%) when compared with GPP_{EC} (Fig. 4, Table 6). MODIS underestimated GPP_{EC} by 9%, on average.

Table 5
Measurements of the accuracy of GPP_{EC} vs. $GPP_{Landsberg}$ (n=122) during the growing season of 2005

Site	RMSE (g C m^{-2} d^{-1})	$RMSE_s$ (g C m^{-2} d^{-1})	$RMSE_u$ (g C m^{-2} d^{-1})	Pearson's correlation coefficient (r) (p)	Spearman's rank correlation (p)
OJP	1.59	1.38	0.75	0.76 (0.000)	–
HJP75	0.66	0.42	0.87	0.86 (0.000)	–
HJP94	0.63	0.46	0.39	0.87 (0.000)	–
HJP02	0.45	0.37	0.26	–	0.28 (0.002)

p-values are included in brackets. Pearson's r correlation is appropriate for OJP, HJP75 and HJP94, whereas Spearman's rank correlation is appropriate for HJP02.

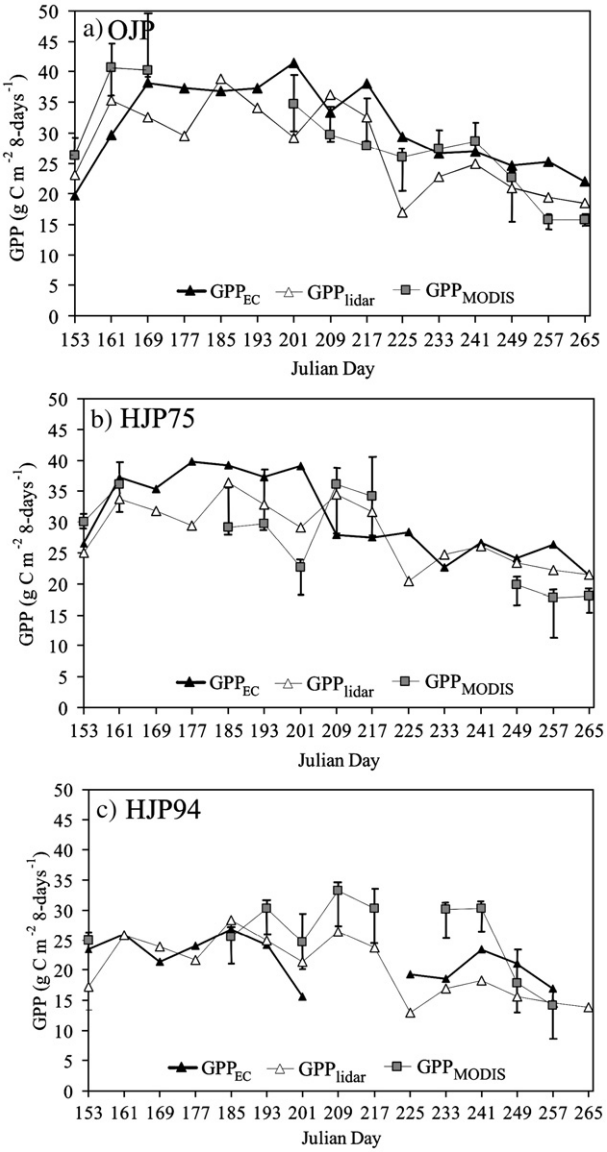

Fig. 4. Eight-day cumulative average GPP comparisons between GPP_{EC}, GPP_{MODIS}, and GPP_{lidar} at a) OJP; b) HJP75; and c) HJP94. Error bars on MODIS data indicate the range of GPP recorded for eight adjacent pixels (to the centre one, nine in total).

When GPP_{MODIS} was compared with GPP_{lidar}, average differences of 6% were found. The standard deviation of differences were greatest between GPP_{EC} and remote sensing estimates (GPP_{lidar}, and GPP_{MODIS}) (16% and 24%, respectively), but were less when comparing between GPP_{lidar} and GPP_{MODIS} (14%).

At HJP94, the footprint area of the EC covers approximately 50% of the MODIS pixel for the site. The remaining 20% and 30% of the pixel contains older jack pine stands with average tree heights of 12 m and 6.5 m, respectively. Tree heights and *f*cover within the MODIS pixel area were also greater (5.2 m, 0.32) than those measured within plots near the tower (Table 1). Average GPP_{lidar} underestimated GPP_{EC} by 6%, especially towards the end of the growing season, whereas GPP_{MODIS} overestimated GPP_{EC} by 17% and GPP_{lidar} by 18% (Fig. 4, Table 6). The standard deviation of the differences were also smallest when comparing GPP_{lidar} with GPP_{MODIS} (17%) but larger when comparing between GPP_{EC} and GPP_{MODIS} (31%).

4.4. Objective 4: assessing the influence of site heterogeneity — scaling GPP from 1 m to 1000 m

From the results of the previous section, it is evident that differences between GPP_{Lidar}, GPP_{MODIS} and GPP_{EC} may depend, in part, on the location and distribution of "patches" of vegetation within mixed pixels. Individual MODIS pixels may include areas of diverse vegetation cover, ranging from recent clearcuts and grasslands, to older and/or more productive forests, wetlands, and agricultural areas (Milne and Cohen, 1999). It is not clear if within-pixel patches have influenced pixel average GPP_{lidar} and GPP_{MODIS} when compared with GPP_{EC}. To examine the influences of spatial heterogeneity in vegetation structure, 1 m resolution GPP_{lidar}, estimated for a single day, was aggregated by averaging to 25 m, 250 m, 500 m, and 1000 m pixel resolutions and then subtracted from 1 m pixels to demonstrate where GPP differences may exist between adjacent patches of vegetation types (Fig. 5).

After aggregating 1 m GPP_{lidar} to lower resolutions, and subtracting them from the original 1 m GPP_{lidar} dataset, GPP_{lidar} was found to vary by almost 10% at the heterogeneous HJP94 site when lower resolutions were used (Table 7). We can start to see the effects of aggregation in Fig. 5a, (3rd panel) at HJP94. Differences between 1 m and 25 m resolutions along the outer edges of the HJP94 site (rectangular area located in the centre of the pixel) were over-estimated by 25 m resolution pixels compared with 1 m resolution pixels, due to edge effects and averaging between taller and shorter vegetation. A *t*-test confirms that significant differences between 1 m and 25 m resolution pixels exist at HJP94 ($p=0.000$, $n=1600$), and to a lesser extent between 1 m and 250 m resolutions ($p=0.10$, $n=16$). The greatest deviations were found at HJP94 at pixel resolutions between 25 m and 500 m, which underestimated average GPP (when compared with 1 m resolution) by up to 10% over the 1 km pixel, and by as much as 5 g C m^{-2} d^{-1} (140%) when compared with 1 m resolutions. These results exemplify the averaging of GPP that occurs as resolution decreases. At HJP75, as pixel resolution decreased to 500 m, pixel average GPP also decreased indicating that short vegetation surrounding the site had some influence on average GPP at lower (e.g. 500 m) resolutions. Slight edge effects at 25 m resolution can be found at HJP75 (Fig. 5a, 2nd panel) between shorter vegetation along the outer edges of the site, and taller vegetation within the site, however, differences between higher and lower pixel resolutions were not significant. Systematic over- and under-estimation of GPP_{lidar} was not found at OJP and average differences between high and low resolution pixels were less than 1.5%. Significant differences at OJP exist between 1 m and 25 m resolution pixels ($p=0.05$, $n=1600$), but not at lower

Table 6
Pearson's *r* correlations between GPP_{EC}, GPP_{lidar}, and GPP_{MODIS} including *p-values* (in brackets)

Site	Pearson's *r* correlation GPP_{EC} and GPP_{lidar}	Average % difference = GPP_{EC} $GPP_{EC}-GPP_{lidar}$	Pearson's r correlation GPP_{EC} and GPP_{MODIS}	Average % difference = GPP_{EC} $GPP_{EC}-GPP_{MODIS}$	Pearson's r correlation GPP_{lidar} and GPP_{MODIS}	Average % difference: = GPP_{lidar} $GPP_{lidar}-GPP_{MODIS}$
OJP	0.71 (0.003)	11%	0.64 (0.030)	6%	0.77 (0.003)	8%
HJP75	0.70 (0.004)	6%	0.39 (0.270)	9%	0.81 (0.004)	6%
HJP94	0.63 (0.280)	6%	0.64 (0.100)	−17%	0.59 (0.04)	−18%

Average percent differences are shown for eight-day composite periods (where data were available) over the growing season, 2005.

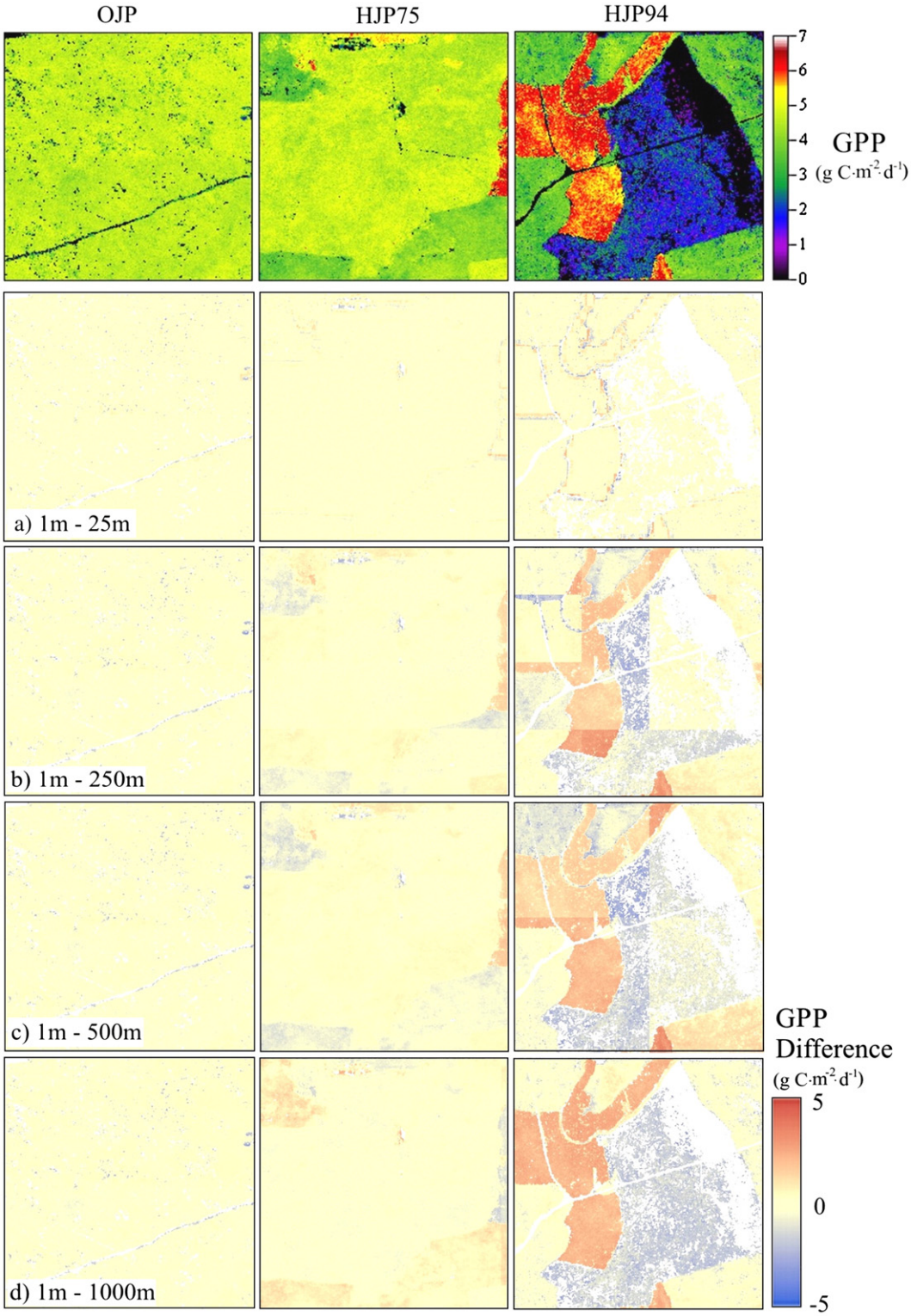

Fig. 5. Differences between GPP_{lidar} on June 16, 2005 (as an example) at 1 m resolution and a) 25 m b) 250 m; c) 500 m; and d) 1000 m pixels. Maps of GPP_{lidar} illustrate more and less productive parts within 1 km×1 km MODIS pixel areas. Low resolution pixels were subtracted from 1 m resolution pixels at each site. Positive differences indicate that lower resolutions underestimate GPP compared with 1 m resolution, whereas negative differences indicate that lower resolutions over-estimate GPP when compared with 1 m resolution. White areas equal missing data due to short vegetation.

resolutions. The effects of pixel averaging at OJP and HJP75 were not great as at HJP94 because these sites are relatively homogeneous and were not subject to large pixel differences as a result of structural heterogeneity. Similar observations have been found in Reich et al. (1999) who show that differences in photosynthetic capacity of vegetation patches can affect the averaging of pixels at lower resolutions.

The results of Fig. 5 and Table 7 provide a good rationale for using low resolution MODIS vegetation products within homogeneous sites, and higher resolution products (e.g. 25 m) within heterogeneous sites.

Table 7
Summary statistics (percent differences) between GPP estimated at 1 m spatial resolution and lower resolutions per site

Site	Difference statistics due to pixel resolution	Pixel resolution (subtracted from 1 m)				
		1 m×1 m	25 m×25 m	250 m×250 m	500 m×500 m	1000 m×1000 m
OJP	Average pixel GPP (g C m^{-2} d^{-1})	4.22	4.21	4.27	4.26	4.22
	Mean % difference from 1 m	0	−0.2	1.2	0.9	0
	Pixel (GPP) standard deviation	0.30	0.24	0.19	0.17	0
HJP75	Average pixel GPP (g C m^{-2} d^{-1})	4.54	4.55	4.55	4.41	4.54
	Mean % difference from 1 m	0	0.2	0.2	−2.8	0
	Pixel (GPP) standard deviation	0.44	0.46	0.59	0.57	0
HJP94	Average pixel GPP (g C m^{-2} d^{-1})	3.65	3.29	3.31	3.31	3.56
	Mean % difference from 1 m	0	−9.9	−9.3	−9.3	−2.5
	Pixel (GPP) standard deviation	1.53	1.52	1.25	1.5	0

Negative signs represent underestimation of GPP by lower resolution pixels.

Depending on the location of patches within pixels, the averaging that occurs within decreasing resolutions may be prone to large and compounding errors in GPP (e.g. Kimball et al., 1999).

5. Discussion

5.1. Influences of site heterogeneity

Low standard deviations in the range of differences between GPP_{lidar} and GPP_{MODIS} indicate the importance of comparing MODIS GPP products over homogeneous pixels where EC systems exist. HJP94 and to a lesser extent, HJP75 are considered "mixed pixels" because they contain some areas of taller and shorter vegetation and variable canopy fractional cover. If applied over an entire MODIS pixel, we expect that GPP_{lidar} and GPP_{MODIS} would be similar because the same pixel area containing the same average vegetation characteristics was used to estimate GPP. In principle, greater differences should exist when comparing predicted GPP (MODIS or lidar) with GPP_{EC} because EC samples only part of the mixed pixel and, therefore, does not represent other landcover types within that pixel. If EC provides only partial coverage of the pixel, then it may be more appropriate to apply a lidar-based or ecosystem model approach over the entire pixel to reduce differences that may be caused by mixed pixels. Alternatively, the spatially variant footprint can be modeled and within footprint lidar-based canopy attributes extracted to scale from point to landscape scales (e.g. Chasmer et al., accepted for publication).

5.2. Other influences affecting MODIS vs. EC GPP

Differences between EC, MODIS and lidar-modeled GPP may also be due to energy balance closure, and biome-specific estimates of LUE and fPAR used by MODIS. EC is prone to underestimating CO_2 fluxes, and differences between GPP_{EC} and GPP estimated using lidar and MODIS may be affected by this. Barr et al. (2006) found that energy balance closure at OJP was 0.86% (±0.003) for daytime periods when friction velocity was greater than 0.35 m s^{-1}. Lack of energy balance closure is sometimes believed to lead to deficits in measured fluxes (Barr et al., 2006; Baldocchi 2008). This uncertainty is minimized, in part, by applying an energy balance correction to the measured fluxes so that deficits are reduced. Baldocchi (2008) suggests that adjusting for energy balance closure may not be appropriate because underestimates in the energy balance may not be manifest in underestimates in CO_2 fluxes. Energy balance correction has been applied to all sites examined in this study (Barr et al., 2006), which may have also increased differences between GPP_{MODIS} and GPP_{EC}.

The use of LUE and estimation of fPAR by MODIS may also introduce additional errors. MODIS typically uses a biome-specific look-up table of LUE, varied with changes in air temperature (Tair) and vapour pressure deficit (VPD) (e.g. Heinsch et al., 2003). However, LUE between vegetation species, age classes, previous disturbance, and meteorological drivers tends to vary greatly (e.g. McCrady and Jokela, 1998; Lagergren et al., 2005; Jenkins et al., 2007; Pereira et al., 2007; Schwalm et al., 2006; Chasmer et al., 2008), despite the simple application of LUE in the MODIS GPP algorithm (Turner et al., 2003). With respect to meteorological driving mechanisms, Jenkins et al. (2007) found that PAR had the greatest influence on measured gross carbon exchanges, whereas Tair and VPD had only weak influences. Lagergren et al. (2005), on the other hand, found the opposite to be true. Chasmer et al. (2008) found that the importance of meteorological drivers on LUE varied with forest age, as did LUE. When applying the MODIS biome-specific estimate for LUE, linearly varied with measured Tair and VPD, Chasmer et al. (2008) found that average growing season LUE was underestimated by 40% at a mature jack pine forest, and between 14% and 16% within younger jack pine stands when compared with measured LUE.

The estimation of fPAR by MODIS could also increase differences between EC-measured GPP and that of MODIS. For example, Turner et al. (2006) found that MODIS underestimated measured GPP in highly productive sites and overestimated measured GPP in low productivity sites. Heinsch et al. (2006) also found that MODIS often over-estimates fPAR, which is used as a multiplier with LUE to estimate GPP. Therefore, low biome-specific estimates of LUE may be used to offset over-estimates of fPAR by the MODIS algorithm (e.g. Zhao et al., 2005; Turner et al., 2006; Heinsch et al., 2006). When compared over an entire watershed (99 MODIS pixels), Chasmer et al. (in press) found that MODIS overestimated fPAR when compared with lidar estimates of the same in approximately 22% of the watershed, especially where pixels contained mixed vegetation with low biomass (e.g. cleared areas). However, in 30% of the watershed, that which contained areas of high biomass, MODIS slightly underestimated fPAR when compared with lidar. These results may also have contributed to the differences between GPP_{MODIS} and GPP_{EC}.

5.3. Implications of this research

The results of this study indicate that airborne scanning lidar is a useful tool for scaling between EC measurements and lower resolution satellite products. Whilst it does not measure the reflective properties of the canopy, which may be directly applicable to MODIS, it does provide information on three-dimensional vegetation structure. The ability to accurately estimate canopy fractional cover and leaf area from lidar within one to many MODIS pixels has many benefits. These include, but are not limited to, continuous scaling of leaf area over varying pixel resolutions, significantly reduced time and costs associated with extensive LAI measurements within and beyond pixels, and the ability to map and discretize the three-dimensional foliage area with depth into the canopy. Running et al. (1999) provide a list of measurements that are useful for validating MODIS using ecosystem models. Several of these can be accurately obtained from airborne lidar and may be incorporated into ecosystem models. These include: a) light transmission (e.g. Solberg et al., 2006; Thomas et al., 2006; Hopkinson and Chasmer, 2007); b) above ground biomass

(Patenaude et al., 2004; Omasa et al., 2007); c) leaf area index (Magnussen and Boudewyn, 1998; Morsdorf et al., 2006; Hopkinson and Chasmer, in review); d) canopy height (Naesset and Bjerknes, 2001; Hopkinson et al., 2005); e) aerodynamic roughness length and zero plane displacement (Chasmer et al., accepted for publication); and f) above-ground growth increment (Yu et al., 2004; Hopkinson et al., 2007). The increasing popularity of lidar, and vast lidar data collection and archiving projects (e.g. the USGS CLICK project, and the Canadian LIMERIC data archive) have made lidar an accessible tool for the evaluation of lower resolution remote sensing products. Repeat surveys and small-area monitoring strategies are also gaining focus (Hopkinson et al., 2007).

Lidar estimates of fractional cover at high resolutions may be combined with incoming PAR (e.g. in this study) and other meteorological driving mechanisms to produce spatial and temporal maps of GPP. If ecosystem production models (e.g. SVAT, Running et al., 1999; Biome BGC, Thornton et al., 2002; 3PGS, Coops et al., 2007), were combined with airborne lidar, the results may provide more appropriately scaled estimates of GPP for MODIS evaluation than EC within mixed pixels. In this study, differences between GPP_{MODIS} and GPP_{lidar} were not as large as differences between GPP_{EC}. This was due, in part, to the same area being compared between MODIS and lidar. Within mixed MODIS pixels, EC samples the ecosystem of interest, and may or may not provide an accurate description of GPP for the entire MODIS pixel (Rahman et al., 2001). If the forest is homogeneous and extends beyond the MODIS pixel, then comparisons between MODIS and EC should be similar, as was shown in this study.

6. Conclusions

In summary, this study describes the application of a canopy structure-based GPP model within both homogeneous and mixed pixels for comparison with the MODIS GPP product. First, canopy height and foliage fractional cover were compared with inputs used in Landsberg light response curves during the growing season of 2004. P_{max} was positively, but non-linearly, related to canopy height. Similar relationships were also found between the canopy structure and both the scaling factor (a) and I_{comp}. A GPP model was created based on the strong relationships found between canopy structure and Landsberg inputs. $GPP_{Landsberg}$ approximated GPP_{EC} at HJP75 and HJP94, but over-estimated GPP_{EC} at OJP and under-estimated GPP_{EC} at HJP02.

Second, we used lidar inputs into the $GPP_{Landsberg}$ model (instead of measured: i.e. GPP_{lidar}) with GPP_{EC} and the GPP_{MODIS} within 1 km×1 km MODIS pixel areas surrounding the EC. When compared over eight-day cumulative periods throughout the 2005 growing season, the standard deviation of differences between GPP_{lidar} and GPP_{MODIS} were less than differences between GPP_{EC} at all sites. Although OJP and HJP75 were relatively homogeneous surrounding the EC system, lower canopy heights and leaf area may have resulted in lower estimates of GPP by lidar and MODIS than measured. At HJP94, MODIS overestimated GPP when compared with EC, possibly due to taller trees with higher leaf area surrounding the site, but outside of the fetch of the EC system. Differences in canopy cover and tree height within and beyond the site did not have the same affect on GPP_{lidar}, which was slightly underestimated towards the end of the growing season.

Finally, we examined the influence of coarser resolutions and within-pixel averaging on GPP_{lidar} at OJP, HJP75, and HJP94. We found that the largest differences occurred at HJP94, especially when aggregating pixels beyond 25 m. This provides a good rationale for using high resolution spatial data in heterogeneous environments. Further, the use of airborne scanning lidar greatly reduces the need for extensive field validation, and is an appropriate method for scaling between EC estimates of GPP and MODIS products.

Acknowledgements

We would like to thank the Fluxnet-Canada Research Network and the Boreal Ecosystem Research and Monitoring Sites (BERMS) Project. The lidar data were collected by the Applied Geomatics Research Group. The National Water Research Institute (NWRI) and the Climate Research Division, Atmospheric Sciences and Technology Directorate, Environment Canada have provided financial support for the lidar survey. Help with field data collection was provided by Bruce Davison, Chris Beasy, and Jordan Erker. Also, thank-you to the late Werner Bauer (site manager) for his help and support. MODIS data were obtained from the Oak Ridge National Laboratory Distributed Active Archive Center (ORNL DAAC). 2005 MODIS subset land products are available on-line [http://www.daac.ornl.gov/MODIS/modis.html] from ORNL DAAC, Oak Ridge, Tennessee, U.S.A. Funding for this project has been provided by CFCAS, NSERC, PREA, the BIOCAP Canada Foundation, and the Climate Research Division of Environment Canada. Laura has been supported by graduate student scholarships from NSERC and OGSST and research assistantships from CRESTech. Finally thank-you for the valuable suggestions provided by two anonymous reviewers.

References

Baldocchi, D. (2008). Turner Review No. 15: 'Breathing' of the terrestrial biosphere: Lessons learned from a global network of carbon dioxide flux measurement systems. *Australian Journal of Botany*, *56*, 1–26.

Baldocchi, D., & Meyers, T. (1998). On using eco-physiological, micrometeorological and biogeochemical theory to evaluate carbon dioxide, water vapor and trace gas fluxes over vegetation: a perspective. *Agricultural and Forest Meteorology*, *90*, 1–25.

Baldocchi, D. D., Vogel, C. A., & Hall, B. (1997). Seasonal variation of carbon dioxide exchange rates above and below a boreal jack pine forest. *Agricultural and Forest Meteorology*, *83*, 147–170.

Barr, A. G., Black, T. A., Hogg, E. H., Kljun, N., Morgenstern, K., & Nesic, Z. (2004). Interannual variability in the leaf area index of a boreal aspen-hazelnut forest in relation to net ecosystem production. *Agricultural and Forest Meteorology*, *126*, 237–255.

Barr, A. G., Morgenstern, K., Black, T. A., McCaughey, J. H., & Nesic, Z. (2006). Surface energy balance closure by the eddy-covariance method above three boreal forest stands and implications for the measurement of the CO2 flux. *Agricultural and Forest Meteorology*, *140*, 322–337.

Burns, R., & Honkala, B. (1990). Silvics *of Forest Trees of the United States*. *Supersedes Agriculture Handbook 271. US Department of Agriculture, Forest Service, Washington DC* PDF copies available on website: http://na.fs.fed.us/pubs/

Chasmer, L., Barr, A., Black, A., Hopkinson, C., Kljun, N., McCaughey, H., Treitz, P., (accepted for publication) Vegetation structural and elevation influences on CO2 uptake within a mature jack pine forest in Saskatchewan Canada. *Canadian Journal of Forest Research*.

Chasmer, L., Hopkinson, C., Smith, B., & Treitz, P. (2006). Examining the influence of changing laser pulse repetition frequencies on conifer forest canopy returns. *Photogrammetric Engineering and Remote Sensing*, *17*(12), 1359–1367.

Chasmer, L., Hopkinson, C., Treitz, P., McCaughey, H., Barr, A., Black, A., (in press). A lidar-based hierarchical approach for assessing MODIS fPAR. *Remote Sensing of Environment*.

Chasmer, L., McCaughey, H., Barr, A., Black, A., Shashkov, A., Treitz, P., et al. (2008). Investigating light use efficiency (LUE) across a jack pine chronosequence during dry and wet years. *Tree Physiology*, *28*(9), 1395–1406.

Chen, J., Falk, M., Euskirchen, E., Paw, K. T., Suchanek, U. T. H., Ustin, S., et al. (2002). Biophysical controls of carbon flows in three successional Douglas-fir stands based on eddy-covariance measurements. *Tree Physiology*, *22*, 169–177.

Chen, J. M., Govind, A., Sonnentag, O., Zhang, Y., Barr, A., & Amiro, B. (2006). Leaf area index measurements at Fluxnet-Canada forest sites. *Agricultural and Forest Meteorology*, *140*, 257–268.

Chen, B., Chen, J., Mo, G., Black, T. A., & Worthy, D. E. (2008). Comparison of regional carbon flux estimates from CO_2 concentration measurement and remote sensing based footprint integration. *Global Biogeochemical Cycles*, *22*(GB2012).

Coops, N. C., Black, T. A., Jassal, R. S., Trofymow, J. A., & Morgenstern, K. (2007). Comparison of MODIS, eddy covariance determined and physiologically modeled gross primary production (GPP) in a Douglas-fir forest stand. *Remote Sensing of Environment*, *107*, 385–401.

Eriksson, H. M., Eklundh, L., Kuusk, A., & Nilson, T. (2006). Impact of understory vegetation on canopy reflectance and remotely sensed LAI estimates. *Remote Sensing of Environment*, *103*, 408–418.

Fluxnet-Canada (2003). Fluxnet-Canada measurement protocols. *Working draft version 1.3. Fluxnet-Canada Network Management Office, Laval, Quebec* Available online: http://www.fluxnet-canada.ca

Heinsch, F. A., Reeves, M., Bowker, C. F., Votava, P., Kang, S., Milesi, C., Zhao, M., Glassy, M., Kimball, J., Nemani, R., & Running, S. W. (2003). *User's Guide, GPP and NPP (MOD17A2/A3, NASA MODIS Land Algorithm*, Version 1.2. www.ntsg.umt.edu/modis/MOD17UsersGuide.pdf

Heinsch, F. A., Zhao, M., Running, S. W., Kimball, J. S., Nemani, R. R., Davis, K. J., et al. (2006). Evaluation of remote sensing based terrestrial productivity from MODIS

using regional tower eddy flux network observations. *IEEE Transactions on Geoscience and Remote Sensing*, *44*(7), 1908–1925.

Hopkinson, C. and Chasmer, L., (in review). Testing a lidar intensity based model of canopy fractional cover across multiple forest ecozones. *Remote Sensing of Environment*.

Hopkinson, C., & Chasmer, L. (2007). Using discrete laser pulse return intensity to model canopy transmittance. *The Photogrammetric Journal of Finland*, *20*(2), 16–26.

Hopkinson, C., Chasmer, L., & Hall, R. (2007). Using airborne lidar to examine forest growth. *Remote Sensing of Environment*, *112*(3), 1168–1180.

Hopkinson, C., Chasmer, L., Sass, G., Creed, I., Sitar, M., Kalbfleisch, W., et al. (2005). Vegetation class dependent errors in lidar ground elevation and canopy height estimates in a boreal wetland environment. *Canadian Journal of Remote Sensing*, *31*(2), 191–206.

Jenkins, J. P., Richardson, A. D., Braswell, B. H., Ollinger, S. V., Hollinger, D. Y., & Smith, L. L. (2007). Refining light-use efficiency calculations for a deciduous forest canopy using simultaneous tower-based carbon flux and radiometric measurements.*Agricultrual and Forest Meteorology* 143-64-79.

Jin, Z., Tian, Q., Chen, J. M., & Chen, M. (2007). Spatial scaling between leaf area index maps of different resolutions. *Journal of Environmental Management*, *85*, 628–637.

Kljun, N., Black, T. A., Griffis, T. J., Barr, A. G., Gaumont-Guay, D., Morgenstern, K., et al. (2006). Response of net ecosystem productivity of three boreal forest stands to drought, 2006. *Ecosystems*, *9*, 1128–1144.

Kimball, J. S., Running, S. W., & Saatchi, S. S. (1999). Sensitivity of boreal forest regional water flux and net primary production simulations to sub-grid scale landcover complexity. *Journal of Geophysical Research*, *104*, 27789–27801.

Lagergren, F., Eklundh, L., Grelle, A., Lundblad, M., Molder, M., Lankreijer, H., et al. (2005). Net primary production and light use efficiency in a mixed conifer forest in Sweden. *Plant, Cell, and Environment*, *28*, 412–423.

Landsberg, J. J., & Waring, R. H. (1997). A generalized model of forest productivity using simplified concepts of radiation-use efficiency, carbon balance and partitioning. *Forest Ecology and Management*, *95*, 209–228.

Leblanc, S. G., Chen, J. M., Fernandes, R., Deering, D., & Conley, A. (2005). Methodology comparison for canopy structure parameters extraction from digital hemispherical photography in boreal forests. *Agricultural and Forest Meteorology*, *129*, 187–207.

Magnussen, S., & Boudewyn, P. (1998). Derivations of stand heights from airborne laser scanner data with canopy-based quantile estimators. *Canadian Journal of Forest Research*, *28*, 1016–1031.

Margolis, H., Flanagan, L., & Amiro, B. (2006). The Fluxnet-Canada Research Network: Influence of climate and disturbance on carbon cycling in forests and peatlands. *Agricultural and Forest Meteorology*, *140*, 1–5.

Massman, W. J., & Lee, X. (2002). Eddy covariance flux corrections and uncertainties in long term studies of carbon and energy exchange. *Agricultural and Forest Meteorology*, *113*, 121–144.

McCrady, R. L., & Jokela, E. (1998). Canopy dynamics, light interception and radiation use efficiency of selected loblolly pine families. *Forest Science*, *44*, 64–72.

Milne, B. T., & Cohen, W. B. (1999). Multiscale assessment of binary and continuous landcover variables for MODIS validation, mapping, and modeling applications. *Remote Sensing of Environment*, *70*, 82–98.

Middleton, E. M., Sullivan, J., Bovard, B., Deluca, A., Chan, S., & Cannon, T. (1997). Seasonal variability in foliar characteristics and physiology for boreal forest species at five Saskatchewan tower sites during the 1994 Boreal Ecosystem-Atmosphere Study. *Journal of Geophysical Research*, *102*(D24), 28831–28844.

Morsdorf, F., Kötz, B., Meier, E., Itten, K., & Allgöwer, B. (2006). Estimation of LAI and fractional cover from small footprint airborne laser scanning data based on gap fraction. *Sensing of Environment*, *104*, 50–61.

Myers, D. E. (1994). Spatial interpolation: An overview. *Geoderma*, *62*, 17–28.

Naesset, E., & Bjerknes, K. O. (2001). Estimating tree heights and number of stems in young forest stands using airborne laser scanner data. *Remote Sensing of Environment*, *78*, 328–340.

Omasa, K., Hosoi, F., & Konishi, A. (2007). 3D lidar imaging for detecting and understanding plant responses and canopy structure. *Journal of Experimental Botany*, *58*(4), 881–898.

O'Sullivan, D., & Unwin, D. (2003). *Geographic information analysis.* New Jersey: Wiley.

Patenaude, G., Hill, R. A., Milne, R., Gaveau, D., Briggs, B., & Dawson, T. (2004). Quantifying forest above ground carbon content using LiDAR remote sensing. *Remote Sensing of Environment*, *93*, 368–380.

Pereira, J. S., Mateus, J. A., Aires, L. M., et al. (2007). Net ecosystem carbon exchange in three contrasting Meterranean ecosystems — The effect of drought. *Biogeosciences*, *4*, 791–802.

Rahman, A., Gamon, J., Fuentes, D., Roberts, D., & Prentiss, D. (2001). Modeling spatially distributed ecosystem flux of boreal forest using hyperspectral indices from AVIRIS imagery. *Journal of Geophysical Research*, *106*(D24), 33579–33591.

Reich, P. B., Turner, D. P., & Bolstad, P. (1999). An approach to spatially distributed modeling of net primary production (NPP) at the landscape scale and its application in validation of EOS NPP products. *Remote Sensing of Environment*, *70*, 69–81.

Running, S. W., Nemani, R., Glassy, J., & Thornton, P. (1999). MODIS daily photosynthesis (Psn) and annual net primary production (NPP) product (MOD17). *Theoretical basis document, Version 3* Greenbelt, MD 20771, USA: NASA Goddard Space Flight Center Available online: http://modis.gsfc.nasa.gov/data/atbd/atbd_mod17.pdf

Rymph, S.J., 2004. Modeling growth and composition of perennial tropical forage grasses. Ph.D. Thesis, University of Florida. 330 pgs.

Schwalm, C. R., Black, T. A., Amiro, B. D., Arain, M. A., Barr, A. G., Bourque, C. P. A., et al. (2006). *Agricultural and Forest Meteorology*, *140*, 269–286.

Solberg, S., Naesset, E., Hanssen, K. H., & Christiansen, E. (2006). Mapping defoliation during a severe insect attack on Scots pine using airborne laser scanning. *Remote Sensing of Environment*, *102*, 364–376.

Thomas, V., Finch, D., McCaughey, J. H., Noland, T., Rich, L., & Treitz, P. (2006). Spatial modeling of the fraction of photosynthetically active radiation absorbed by a boreal mixedwood forest using a lidar-hyperspectral approach. *Agricultural and Forest Meteorology*, *140*, 287–307.

Thornton, P., Law, B. E., Gholz, H., Clark, K., Falge, E., Ellsworth, D., et al. (2002). Modelling and measuring the effects of disturbance history and climate on carbon and water budgets in evergreen needle leaf forests. *Agricultural and Forest Meteorology*, *113*(1–2), 185–222.

Tian, Y., Woodcock, C., Wang, Y., Privette, J., Shabanov, N., Zhou, L., et al. (2002). Multiscale analysis and validation of the MODIS LAI product 1. Uncertainty assessment. *Remote Sensing of Environment*, *83*, 414–430.

Turner, D. P., Gower, S. T., Cohen, W. B., Gregory, M., & Maiersperger, T. K. (2002). Effects of spatial variability in light use efficiency on satellite-based NPP monitoring. *Remote Sensing of Environment*, *80*, 397–405.

Turner, D. P., Ollinger, S., & Kimball, J. (2004). Integrating remote sensing and ecosystem process models for landscape- to regional-scale analysis of the carbon cycle. *BioScience*, *54*(6), 573–584.

Turner, D. P., Ritts, W. D., Cohen, W. B., Gower, S. T., Running, S. W., Zhao, M., et al. (2006). Evaluation of MODIS NPP and GPP products across multiple biomes. *Remote Sensing of Environment*, *102*, 282–292.

Turner, D. P., Urbanski, S., Bremer, D., Wofsy, S. C., Meyers, T., Gower, S. T., et al. (2003). A cross-biome comparison of daily light use efficiency for gross primary production. *Global Change Biology*, *9*, 383–395.

Wolfe, R. E., Nishihama, M., Fleig, A. J., Kuyper, J. A., Roy, D. P., Storey, J. C., et al. (2002). Achieving sub-pixel geolocation accuracy in support of MODIS land science. *Remote Sensing of Environment*, *83*, 31–49.

Woolard, J., & Colby, J. (2002). Spatial characterization, resolution, and volumetric change of coastal dunes using airborne lidar: Cape Hatteras, North Carolina. *Geomorphology*, *48*(1–3), 269–287.

Xu, S., Chen, J. M., Fernandes, R., & Cihlar, J. (2004). Effects of subpixel water area fraction on mapping leaf area index and net primary productivity in Canada. *Canadian Journal for Remote Sensing*, *30*, 797–804.

Yu, X., Hyyppä, J., Kaartinen, H., & Maltamo, M. (2004). Automatic detection of harvested trees and determination of forest growth using airborne laser scanning. *Remote Sensing of Environment*, 90451–90462.

Zhang, Y., Chen, J., & Miller, J. (2005). Determining digital hemispherical photograph exposure for leaf area index estimation. *Agricultural and Forest Meteorology*, *133*, 166–181.

Zhao, M., Heinsch, F. A., Nemani, R. R., & Running, S. (2005). Improvements of the MODIS terrestrial gross and net primary production global data set. *Remote Sensing of Environment*, *95*, 164–176.